Diffusion and sorption of organic micropollutants in biofilms with varying thicknesses

Elena Torresi[1,2†**], Fabio Polesel[1†***], Kai Bester[3], Magnus Christensson[2], Barth F. Smets[1], Stefan Trapp[1], Henrik R. Andersen[1], Benedek Gy. Plósz[1,4]*

[1]DTU Environment, Technical University of Denmark, Bygningstorvet B115, 2800 Kongens Lyngby, Denmark

[2]Veolia Water Technologies AB, AnoxKaldnes, Klosterängsvägen 11A, SE-226 47 Lund, Sweden

[3]Department of Environmental Science, Århus University, Frederiksborgvej 399, 4000 Roskilde, Denmark

[4]Department of Chemical Engineering, University of Bath, Claverton Down, Bath BA2 7AY, UK

† The authors equally contributed to this manuscript.

*Benedek Gy. Plósz: b.g.plosz@bath.ac.uk

**Elena Torresi: elto@env.dtu.dk

***Fabio Polesel: fabp@enf.dtu.dk

Abstract

Solid-liquid partitioning is one of the main fate processes determining the removal of micropollutants in wastewater. Little is known on the sorption of micropollutants in biofilms, where molecular diffusion may significantly influence partitioning kinetics. In this study, the diffusion and the sorption of 23 micropollutants were investigated in novel moving bed biofilm reactor (MBBR) carriers with controlled biofilm thickness (50, 200 and 500 µm) using targeted batch experiments (initial concentration=1 µg L^{-1}, for X-ray contrast media 15 µg L^{-1}) and mathematical modelling. We assessed the influence of biofilm thickness and density on the dimensionless effective diffusivity coefficient f (-, equal to the biofilm-to-aqueous diffusivity ratio) and the distribution coefficient $K_{d,eq}$ (L g^{-1}). Sorption was significant only for eight positively charged micropollutants (atenolol, metoprolol, propranolol, citalopram, venlafaxine, erythromycin, clarithromycin and roxithromycin), revealing the importance of electrostatic interactions with solids. Sorption equilibria were likely not reached within the duration of batch experiments (4 h), particularly for the thickest biofilm, requiring the calculation of the distribution coefficient $K_{d,eq}$ based on the approximation of the asymptotic equilibrium concentration (t > 4 h). $K_{d,eq}$ values increased with increasing biofilm thickness for all sorptive micropollutants (except atenolol), possibly due to higher porosity and accessible surface area in the thickest biofilm. Positive correlations between $K_{d,eq}$ and micropollutant properties (polarity and molecular size descriptors) were identified but not for all biofilm thicknesses, thus confirming the challenge of improving predictive sorption models for positively charged compounds. A diffusion-sorption model was developed and calibrated against experimental data, and estimated f values also increased with increasing biofilm thickness. This indicates that diffusion in thin biofilms may be strongly limited ($f \ll 0.1$) by the high biomass density (reduced porosity).

Keywords: Pharmaceuticals, wastewater, moving bed biofilm reactor, partitioning, biofilm density, ionizable chemicals

1. Introduction

In wastewater treatment systems, partitioning of organic micropollutants to solid matrices is one of the mechanisms leading to their removal from the aqueous phase. The extent of partitioning is typically compound-dependent, and is governed by its affinity for organic phase (i.e., hydrophobic partitioning) and/or by electrostatic and other similar interactions between ionized molecules and charged solid surfaces (i.e., non-hydrophobic partitioning) (Franco and Trapp, 2008; Hyland et al., 2012; Ternes et al., 2004; Mackay and Vasudevan, 2012; Polesel et al., 2015).

Partitioning describes the distribution of molecules between the aqueous and the solid phase. At equilibrium, sorption and desorption rates are equal, and the ratio of sorbed and dissolved concentrations—normalized to the concentration of solids—is defined as the (linear) solid-liquid partition coefficient K_d (expressed in units of L kg^{-1} or, alternatively, L g^{-1}) (Joss et al., 2006; Ternes et al., 2004). Non-linear expressions (Freundlich and Langmuir isotherms) have been also used to describe partitioning equilibria to account for saturation of solid surfaces or synergistic effects (Delle Site, 2001).

Solid-liquid partitioning has been characterized for activated sludge biomass for a high number of pharmaceuticals Considerably less evidence is available for wastewater treatment biofilms, being limited to antibiotics (sulfamethoxazole, erythromycin, ciprofloxacin, tetracycline) and psycho-active drugs (fluoxetine) in biofilters (Wunder et al., 2011) and granules (Alvarino et al., 2015; Shi et al., 2011). Additionally, partitioning kinetics of other organic contaminants (polycyclic aromatic hydrocarbons, estrogens, nonylphenols, biocides) have been assessed for pure culture biofilms (Wicke et al., 2008, 2007) and river biofilms (Headley et al., 1998; Writer et al., 2011).

Although considered a fast process, partitioning is influenced by mass transfer limitation through diffusive boundary layers and inside the solid matrices, which likely determines the

time needed to achieve equilibrium between aqueous and sorbed concentrations (Joss et al., 2004, 2006). While for activated sludge the equilibrium time is sufficiently fast to prevent an empirical evaluation of mass transfer limitation (Joss et al., 2004; Plósz et al., 2010; Barret et al., 2011), molecular diffusion may have a major role in determining partitioning kinetics in biofilms. Biofilm characteristics such as biomass density and porosity have been found to influence intra-biofilm diffusion of a number of organic and inorganic chemical compounds. This effect has been described by introducing a coefficient *f*, defined as the ratio of effective diffusivity in biofilms and in free aqueous media, thus defining diffusivity reduction in biofilms (Fan et al., 1990; Guimerà et al., 2016; Horn and Morgenroth, 2006; Trapp and Matthies, 1998; Zhang and Bishop, 1994a). While *f* was determined for a number of organic and inorganic chemical compounds, no conclusive evidence currently exists for organic micropollutant diffusion in biofilms, which was therefore investigated in this study.

In our previous work (Torresi et al., 2016), we investigated the biological transformation of pharmaceuticals in nitrifying moving bed biofilm reactors (MBBRs) using novel MBBR carriers (AnoxKaldnes Z-carriers), allowing the control of the biofilm thickness.

In this study, the main objective set was to assess how the diffusion and partitioning of 23 selected pharmaceuticals vary at different biofilm thicknesses (50, 200 and 500 µm) and to quantify corresponding single point K_d values at environmentally relevant concentration levels. By developing and calibrating a model that describes diffusive transport and partitioning in biofilms, we aimed at elucidating the influence of biofilm thickness on (i) the molecular diffusion of micropollutants within biofilm matrix, described by the dimensionless effective diffusivity coefficient *f*; (ii) the extent of partitioning, described by coefficient K_d. Additionally, using experimental and modelling results, the influence of biofilm characteristics (porosity, density) and molecular properties (e.g., hydrophobicity, ionization) on the mass

99 transfer limitation and sorption of micropollutants in biofilms were assessed.

2. Model development

2.1 Conceptual approach for diffusion and sorption in biofilms and model implementation

Considering molecular diffusion of dissolved micropollutants from the bulk aqueous phase into biofilms as the dominant mechanism (Zhang and Bishop, 1994a), the partitioning of organic micropollutants consists of three consecutive steps (Joss et al., 2004): (1) diffusion of dissolved micropollutant from bulk aqueous phase, through a boundary layer, into the biofilm matrix; (2) diffusion of dissolved micropollutant through the biofilm matrix via its pores; (3) sorption to the solid phase of the biofilm matrix (Fig. 1a). The diffusivity of organic chemicals in a free aqueous medium ($D_{W,i}$, $m^2\ d^{-1}$) can be predicted from properties of the chemical (e.g., molar volume) and of the medium. In this study, $D_{W,i}$ values for each chemical were calculated according to Hayduk and Laudie (1974), although alternative approaches were also tested (Table S1 in Supplementary Information).

Transport from the bulk liquid to the biofilm is controlled by the diffusion rate through a boundary layer, for which the diffusivity was assumed equal to $D_{W,i}$ (**Assumption I**, Fig 1b). The thickness of the boundary layer, L_L (μm), was assumed to be equal to 10 μm for all the Z-carriers (Brockmann et al., 2008, see section 1 in SI). In biofilms, molecular diffusivity is reduced compared to free aqueous media (Wanner and Reichert, 1996). This has been attributed to the "tortuosity" of the transport path in biofilms, i.e. the increased (non-linear) path length needed for diffusive transport as compared to free aqueous media (Zhang and Bishop, 1994b). Molecular diffusivity reduction is described by the dimensionless coefficient f, resulting in Eq. 1:

$$D_{bf,i} = f \cdot D_{W,i} \qquad \text{(Eq. 1)}$$

where $D_{bf,i}$ (m^2 d^{-1}) is the effective diffusivity of micropollutants within biofilms and f (-) is always lower than 1. While f values of 0.5–0.8 have been assigned for micropollutant diffusion (Ort and Gujer, 2008; Vasiliadou et al., 2014), this parameter is likely to vary significantly depending on the biofilm structure and properties (biofilm thickness, density, porosity and tortuosity).

It has previously been shown that biofilm porosity and density can vary over the biofilm depth (Zhang and Bishop, 1994a). In the model, we assume the biofilm as a homogenous porous medium (**Assumption II**), although we accept that biofilms with different depth can have different average porosities and densities. As a consequence, only one f value was used to describe diffusion reduction into a biofilm with a certain thickness.

Sorption/desorption kinetics were described using first-order rate equations (see matrix in Fig. 1c). Sorption was considered as an equilibrium process (**Assumption III**), by attributing an arbitrarily high value to the desorption rate k_{des}, thereby making diffusion from the bulk aqueous phase and within the biofilm the rate-limiting steps for solid-liquid partitioning. At micropollutant concentration levels targeted in this study (ng L^{-1} to µg L^{-1}), sorption can be considered linear and better described by the distribution coefficient K_d (**Assumption IV**).

Based on the presented conceptual approach, a diffusion-sorption model was implemented as one-dimensional biofilm model in Aquasim 2.1 (Reichert, 1994). Design and measured biofilm properties (biofilm thickness, surface area, biomass density, porosity) were used as input to the model (see Table 1). Each biofilm was spatially discretized in 20 completely mixed layers. This allowed solving the generic mass balance equation for dissolved micropollutant concentration C_L (ng L^{-1}) in biofilm (Eq. 2):

$$\frac{\partial C_L}{\partial t} = D_{bf,i}\frac{\partial^2 C_L}{\partial z^2} - k_{des}K_d C_L X + k_{des}C_S \qquad \text{(Eq. 2)}$$

(where X is the biomass concentration in biofilm, g L^{-1}; C_S is the sorbed micropollutant concentration, ng L^{-1}; C_L varies with time t and depth z) as a set of ordinary differential equations by using the method of lines (Wanner and Reichert, 1996). According to the diffusion-sorption model, micropollutants undergo equilibrium microscale partitioning as they diffuse through biofilm, in analogy to the approach proposed by Wu and Gschwend (1986). Further details on the conceptual biofilm model, on microscopic mass balances and on the initial conditions are given in the Supplementary Information (section S1 and Figure S1).

< Figure 1 >

2.2 Calculation of sorption coefficients

At equilibrium, the micropollutant concentration sorbed onto biomass ($C_{S,eq}$, µg L^{-1}) is proportional to the dissolved concentration ($C_{L,eq}$, µg L^{-1}), and their ratio, normalized by the concentration of solids ($X_{biomass}$, g L^{-1}), is used to calculate the sorption coefficient K_d (L g^{-1}). With negligible transformation, it is commonly assumed (e.g., in activated sludge) that the sorbed concentration is equivalent to the decrease in dissolved concentration ($C_{L,0} - C_{L,eq}$) between the beginning and the end of batch sorption experiments.

When considering biofilm systems, transport in biofilm pores, along with sorption, can also determine a decrease of micropollutant concentrations in the bulk phase. Hence, the coefficient $\boldsymbol{K_{d,eq}}$ (L g^{-1}) was defined to describe sorption in Z-carrier biofilms based on mass balance considerations (Eq. 3):

$$K_{d,eq} = \frac{\left[\frac{C_{L,0}V_{bulk}}{V_{bulk}+V_{bf,wet}} - \frac{C_{L,eq}(V_{bulk}+V_{PW})}{V_{bulk}+V_{bf,wet}}\right]}{C_{L,eq}X_{biomass}} \qquad \text{(Eq. 3)}$$

where V_{bulk} (L) denotes the volume of the bulk liquid, $V_{bf,wet}$ (L) the volume of wet biofilm (equal to the total surface area of Z-carriers times the defined biofilm thickness) and V_{PW} (L)

169 the volume of the pore water in the biofilm matrix, not accounting for cellular water content
170 (see 3.4). The procedure used to derive Eq. 3 is presented in detail in the Supplementary
171 Information (section S3).
172 The 'asymptotic' concentration $C_{L,eq}$, defining true sorption equilibrium, was estimated by
173 fitting measured concentration profiles in batch sorption experiments with a first-order decay
174 equation (Eq. 4)

175 $$C_L(t) = (C_{L,0} - C_{L,eq})e^{-kt} + C_{L,eq} \quad \text{(Eq. 4)}$$

176 In activated sludge, it has been widely accepted that sorption equilibrium can be reached
177 within 0.5–1 h (Ternes et al., 2004; Andersen et al., 2005; Yi and Harper, 2007, Hörsing et al.,
178 2011). To verify whether sorption equilibrium was achieved relatively fast (i.e., within the 4-
179 hour duration of sorption experiments) also in Z-carrier biofilms, the sorption coefficient $\boldsymbol{K_{d,4h}}$
180 (L g^{-1}) was calculated (Eq. 5):

181 $$K_{d,4h} = \frac{\left[\frac{C_{L,0}V_{bulk}}{V_{bulk}+V_{bf,wet}} - \frac{C_{L,4h}(V_{bulk}+V_{PW})}{V_{bulk}+V_{bf,wet}}\right]}{C_{L,4h}X_{biomass}} \quad \text{(Eq. 5)}$$

182 where $C_{L,4h}$ is the measured dissolved concentration in bulk aqueous phase at t=4 h (the last
183 measurement in sorption experiments), replacing $C_{L,eq}$ in Eq. 3. Specifically, the 4-hour
184 equilibrium assumption was verified by comparing $K_{d,4h}$ and $K_{d,eq}$ and assessing the relative
185 deviation between the two coefficients.
186 As mentioned above, the decrease of bulk micropollutant concentration during sorption
187 experiments with biofilms results from transport in biofilm pores (besides sorption in
188 biofilms). To verify the impact of neglecting mass transfer to biofilm pores on sorption
189 coefficient determination, the sorption coefficient $\boldsymbol{K_{d,susp}}$ was calculated (Eq. 6):

190 $$K_{d,susp} = \frac{C_{L,0} - C_{L,eq}}{C_{L,eq}X_{biomass}} \quad \text{(Eq. 6)}$$

where $C_{L,eq}$ was calculated using Eq. 4. Notably, Eq. 6 is commonly used to describe sorption onto suspended activated sludge, where the effect of porosity is neglected. The comparison between $K_{d,eq}$ and $K_{d,susp}$ (together with relative deviation the two coefficients) was used to quantify the contribution of transport to biofilm pores, hence the impact of porosity, on the estimated sorption coefficient.

2.3 Parameter estimation approach

The assessment of diffusion and sorption of micropollutants in biofilms consisted of two main consecutive steps performed for each micropollutant and at different biofilm thicknesses: (i) calculation of the coefficient $K_{d,eq}$ (section 2.2); (ii) calibration of the diffusion-sorption model (section 2.1) against experimental data and estimation of the coefficient f, which was the only parameters fitted in the model. Estimation of f was performed using the secant model calibration algorithm embedded in Aquasim 2.1.

3. Materials and methods

3.1. System description and operation

Nitrifying MBBRs used in this study have been described elsewhere (Torresi et al., 2016). Briefly, two laboratory-scale nitrifying MBBRs were operated in parallel under continuous-flow conditions for approximately 300 days. Z-carriers (AnoxKaldnes AB, Lund, Sweden) were used to obtain biofilm of different thicknesses. Z-carriers have a saddle shaped grid covered surface allowing for biofilm growth only up to the height of the grid wall (Torresi et al., 2016). Three different Z-carriers (named Z50, Z200, and Z500) were used in this study, with the numbers indicating the grid wall height in μm (hence the maximum controlled biofilm thickness). Biofilms were enriched by feeding the MBBRs with effluent wastewater from a local municipal treatment plant (Källby, Lund, Sweden), spiked with ammonium (50 mg L^{-1} of NH_4-N as NH_4Cl) and phosphate (0.5 mg L^{-1} of PO_4-P as KH_2PO_4). The MBBRs were operated under similar conditions, i.e. hydraulic residence time of 2 h, dissolved oxygen concentration of 4.5 ± 0.5 mg L^{-1}, pH of 7.5 ± 0.5 and temperature of 20°C (achieved using a thermostat).

3.2. Sorption batch experiments

Sorption batch experiments were performed after reaching stable nitrogen removal (Torresi et al., 2016), roughly, around day 300. Prior to batch experiments, the two MBBRs were disconnected and three types of Z-carriers (Z50, Z200, Z500) were manually separated. Subsequently, Z-carriers were left overnight at 4°C in a beaker with tap water to allow for desorption of micropollutants possibly sorbed during continuous-flow operation.

Sorption batch experiments were carried out in three 200-mL glass beakers using filtered (0.2 μm Munktell MG/A glass fiber filters) effluent wastewater from Källby treatment plant. Ammonium and nitrate in the feed were at concentration of <0.5 mgN L^{-1} and 6 mgN L^{-1},

228 respectively, while organic carbon concentration was lower than 35 mgCOD L^{-1}, mostly in
229 inert form.
230 The biomass concentration in the three glass beakers was adjusted to 0.8 g L^{-1} based on
231 attached biomass concentration measurements for the different carriers and adjusting the
232 number of carriers accordingly (56 carriers for Z50, 32 for Z200 and 16 for Z500), resulting in
233 a total biofilm surface area of 0.06, 0.04, 0.02 m^2 for the batch containing Z50, Z200 and Z500
234 carriers, respectively. Other abiotic removal processes, such as volatilization, sorption of
235 micropollutants on plastic carriers and glass wall, had been previously assessed and found
236 negligible in MBBRs (Torresi et al., 2016).
237 Twenty-three micropollutants were spiked in all the beakers with an initial concentration of 1
238 µg L^{-1} except for X-ray contrast media (15 µg L^{-1}), as they are usually found at higher
239 concentrations in effluent wastewater (Margot et al., 2015). A stock solution, containing
240 micropollutants dissolved in methanol (40 mg L^{-1}), was first spiked into empty glass beakers
241 and the methanol was allowed to evaporate in the fumehood for approximately 1 hour.
242 Subsequently, the solution was resuspended in filtered effluent for approximately 30 min to
243 dissolve the spiked micropollutants. Biomass inactivation was achieved by: (i) addition of
244 allylthiourea (ATU, 10 mg L^{-1}, Tran et al., 2009; Khunjar and Love, 2011) and nitrogen
245 sparging (Hamon et al., 2014) to inhibit nitrfyng bacteria; and (ii) addition of sodium azide
246 (0.5 g L^{-1}; Rattier et al., 2014) to inhibit the activity of heterotrophic bacteria.
247 The experiment duration was set to 4 hours. Homogenous aqueous samples were collected at
248 regular intervals from the bulk phase in each beaker at 0, 5, 10, 30, 90 and 240 min. The batch
249 experiments were performed at ambient temperature and initial pH was measured to be 7.5 ±
250 0.5. Since only one spiking concentration was tested, results from sorption experiments were
251 used to determine single point K_d values.

252

253 ***3.3. Chemicals***

254 Twenty-three environmentally relevant micropollutants were selected for this study. The
255 targeted pharmaceuticals were grouped in six categories according to their use: (i) four beta-
256 blocker pharmaceuticals (atenolol, metoprolol, propranolol and sotalol); (ii) five X-ray contrast
257 media (diatrizoic acid, iohexol, iopamidol, iopromide, iomeprol); (iii) three sulfonamide
258 antibiotics (sulfadiazine, sulfamethizole and sulfamethoxazole), one metabolite (acetyl-
259 sulfadiazine) and one combination product (trimethoprim); (iv) three non-steroidal anti-
260 inflammatory pharmaceuticals (phenazone, diclofenac, ibuprofen); (v) three psycho-active
261 drugs (carbamazepine, venlafaxine and citalopram); (vi) three macrolide antibiotics
262 (erythromycin, clarithromycin and roxithromycin). Further information regarding chemical
263 structure and properties, CAS numbers and chemical suppliers can be found in Table S2–S3
264 and in Escolà Casas et al. (2015).

265

266 ***3.4. Analytical methods***

267 Samples for micropollutant analysis were collected (4 mL) and analysed via direct injection
268 using internal standards (injected volume of 100 μL). Details regarding sample preparation,
269 internal standards, HPLC and mass spectrometry conditions, limits of detection and
270 quantification are shown in Escolà Casas et al. (2015). Biomass concentration on Z-carriers was
271 measured in two ways: (i) as attached biomass concentration (expressed as total attached
272 solids, TAS), calculated from the difference in weight of three dried carriers (105^{o}C for > 24 h)
273 before and after biofilm removal (using 2M H_2SO_4 with subsequent brushing) (see also Escolà
274 Casas et al., 2015; Falås et al., 2013; Torresi et al., 2016); and (ii) by scraping and suspending
275 the biofilm in tap water and measuring total suspended solids (TSS) and volatile suspended

276 solids (VSS) according to APHA standard methods (Clesceri, 1989). Biofilm properties such
277 as biofilm dry density ρ_d (g cm^{-3}), biomass density in wet biofilm ρ (kg m^{-3}) and porosity ε (%)
278 were calculated according to Tchobanoglous et al. (2003) and Hu et al. (2013) using measured
279 biofilm properties (e.g., solids content), as detailed in the Supplementary Information (section
280 S2). Porosity is defined as the fraction of the biofilm volume occupied only by water outside
281 the cells and not inside the cells (Hu et al., 2013). Furthermore, ρ_d denotes the dry mass of
282 biofilm per volume of dry biofilm (i.e., defines a *true* density) while ρ denotes the dry mass of
283 biomass per volume of wet biofilm (i.e., defines a concentration of biomass within the
284 biofilm). Further discussion on the calculation methodology used and on the biofilm properties
285 can be found in section S2.
286
287 ***3.5. Statistical analysis and influence of chemical properties***
288 Pearson's and Spearman's correlations between $K_{d,eq}$ and chemical properties (expressed in
289 logarithmic base) were assessed at different biofilm thicknesses. A significance level of 0.05
290 was used for all statistical tests in this study. The investigated physico-chemical properties
291 include: the molecular volume *MV* (cm^3 mol^{-1}); the dissociation constant(s) pK_a; the number of
292 rotable bonds (*nRB*); the van der Waals area (*vdWA*, m^2 $kmol^{-1}$) (Sathyamoorthy and
293 Ramsburg, 2013); McGowan's approximation of the molecular volume (V_X, cm^3 mol^{-1}) (Droge
294 and Goss, 2013a); and the topological polar surface area (*TPSA,* $Å^2$) (Mannhold, 2008).
295 Chemical properties and $K_{d,eq}$ were log transformed (Vasudevan et al., 2009) with exception of
296 *nRB* (Sathyamoorthy and Ramsburg, 2013) and molecular size descriptors *MV* and V_X.
297 Chemical properties for each compound were retrieved using ACD/Labs predictions and the
298 database Mol-inisticts (for log*vdWA*) or calculated based on previously defined equations (for
299 V_X: Abraham and McGowan, 1987). Pearson's and Spearman's correlations and their

300 significance were assessed using GraphPad Prism 5.0. Furthermore, possible correlations
301 between f and the abovementioned properties were also investigated. Significant differences
302 between estimated f values for each chemical at different biofilm thickness were determined by
303 examining the overlap between standard deviations of the estimate (Cumming et al., 2007)

4. Results and discussion

4.1. Biofilm properties

Measured and calculated values for a number of biofilm properties are reported in Table 1. Dry biofilm mass per surface area of carrier (gTAS m^{-2}, Table 1) increased with biofilm thickness, being approximately four times higher in Z500 compared to Z50. Biofilm thickness in Z-carriers was recently measured using optical coherence tomography (OCT), revealing good agreement between measured and nominal thickness based on carrier design (Piculell et al., 2016). Conversely, biofilm density in wet biofilm ρ (section 1 in SI) in Z50 was up to 3-fold higher as compared to Z200 and Z500. This suggests a change in biofilm porosity as a function of biofilm thickness. Biofilm porosity ε (Eq. S12), ranged from 75% (Z50) to 93% (Z500) (Table 1). An approximate porosity of 80% is commonly assumed in one-dimensional biofilm models (Wanner and Reichert, 1996; Brockmann et al., 2008) and similar values have been previously determined using modelling approximations (Zacarias et al., 2005; Zhang and Bishop, 1994b). The observed increasing ε with biofilm thickness is in agreement with previous findings for Z-carrier biofilms (Piculell et al., 2016), although lower porosities (approximately of 10 and 30% for Z50 and Z400) were estimated using OCT. Values of biofilm dry density ρ_d (Table 1) for the three biofilms were comparable to that shown in literature (Hu et al., 2013), indicating a higher content of fixed solids in Z500.

< Table 1 >

4.2. Sorption coefficients in biofilms

Sorption was considered significant when a relative concentration drop $(C_{L,0} - C_{L,4h})/C_{L,0}$ higher than 10% was observed (Hörsing et al., 2011), thus accounting for analytical

327 uncertainty. Profiles of aqueous concentration of the sorptive micropollutants measured during
328 batch experiments are shown in Fig. 3 (duplicate measurement) and in Fig. S2.
329 Out of the 23 targeted compounds, sorption was significant only for eight micropollutants,
330 namely atenolol, metoprolol, propranolol, citalopram, venlafaxine, erythromycin,
331 clarithromycin and roxithromycin. The presence of chemicals not exhibiting sorption (e.g.,
332 diclofenac and the targeted sulfonamides) suggests that biomass was successfully inhibited
333 during batch experiments, as most targeted compounds were significantly biodegraded in the
334 same MBBRs without biomass inhibition (Torresi et al. 2016). Interestingly, micropollutants
335 that were positively charged (>90% cationic fraction) at the experimental pH of 7.5 presented
336 significant sorption, with exception of sotalol and trimethoprim. Higher sorption potential of
337 positively charged compounds compared to negatively charged or neutral compounds was
338 previously observed for activated sludge biosolids (Stevens-Garmon et al., 2011; Polesel et al.,
339 2015) and soil (Franco and Trapp, 2008).
340
341 *4.2.1. Sorption coefficients $K_{d,eq}$ and comparison with activated sludge*
342 Sorption coefficients $K_{d,eq}$ in Z50, Z200 and Z500 biofilms were calculated for the above listed
343 cationic micropollutants (Table 2). $K_{d,eq}$ values were compared with previously found sorption
344 coefficients in activated sludge, for which the large majority of micropollutant sorption data
345 are available.
346 **< Table 2 >**
347 Values of $K_{d,eq}$ for atenolol at all the three biofilm thickness were up to 2-fold higher than
348 literature values (Radjenović et al., 2009; Stevens-Garmon et al., 2011), while values in Z50
349 and Z200 were comparable with findings for secondary sludge (Hörsing et al., 2011). As
350 atenolol presents similar molecular properties to other beta-blockers (e.g., molecular weight,

351 pK_a), the reasons behind this high sorption potential are unclear. As to metoprolol, $K_{d,eq}$ values
352 in Z50, Z200 and Z500 were comparable to previously measured coefficients in activated
353 sludge biomass (Maurer et al., 2007; Sathyamoorthy et al., 2013). Similarly to previous
354 studies, propranolol exhibited the highest sorption potential of all selected beta-blockers
355 (Maurer et al., 2007; Radjenović et al., 2009). Notably, a fourth targeted beta blocker sotalol
356 did not show any significant sorption, in agreement with previous findings in activated sludge
357 (Maurer et al., 2007; Sathyamoorthy et al., 2013).
358 Values of $K_{d,eq}$ for Z50 and Z200 were comparable with previous studies on conventional
359 activated sludge and membrane bioreactor (MBR) sludge for clarithromycin (Abegglen et al.,
360 2009; Göbel et al., 2005), erythromycin (Radjenović et al., 2009; Xue et al., 2010) and
361 roxithromycin (Abegglen et al., 2009; Hörsing et al., 2011). On the contrary, $K_{d,eq}$ for Z500
362 differed by one order of magnitude from previously reported values. Nevertheless, 50–80% of
363 dissolved clarithromycin and roxithromycin sorbed on MBR sludge (Abegglen et al., 2009),
364 similarly to clarithromycin and erythromycin in this study (~80%). Furthermore, highly
365 variable macrolide sorption was shown in soil and onto humic acids (Sibley and Pedersen,
366 2008; Uhrich et al., 2014), with estimated K_d values also higher than 8 L g^{-1} or 20 L g^{-1},
367 respectively. Macrolides exhibited the highest $K_{d,eq}$ of all sorptive compounds in Z500 but not
368 at lower biofilm thickness (Table 2). This might be related to the low porosity of the biofilms
369 Z50 and Z200. According to Lipinksi's rule of five (Lipinski et al., 1997), macrolides are
370 expected to poorly permeate across cell membranes and thus to move only in the intracellular
371 space (depending on the porosity) due to their high molecular weight (>500 g mol^{-1}).
372 Furthermore, macrolides are mainly excreted in feces (Göbel et al., 2005) and due to
373 protonation of the tertiary amino group, strong ionic interaction of macrolides with the
374 negatively charged surface of the biomass could be expected.

375 Few studies investigated the sorption of the antidepressant venlafaxine and the antiepileptic
376 citalopram. While sorption coefficients for Z50 and Z200 for both compounds are in agreement
377 with existing literature on activated sludge (Hörsing et al., 2011), higher values were found in
378 Z500 for citalopram.
379 In general, sorption coefficients of all the compounds at the three biofilm thicknesses were
380 comparable or higher than values observed with activated sludge biomass. Studies comparing
381 sorption onto MBR sludge and conventional activated sludge biomass (Joss et al., 2006;
382 Abegglen et al., 2009; Reif et al., 2011; Yi and Harper, 2007) revealed a sorption enhancement
383 in the former case. Increased sorption was associated to the smaller size of MBR sludge flocs
384 (assumed to be around 80–300 μm in diameter), thus resulting in higher accessible surface area
385 (Tchobanoglous et al., 2003). In analogy with MBR sludge, it can be postulated that the high
386 accessible surface area in Z-carrier biofilms (related to the biofilm porous structure) may
387 explain the increased sorption capacity of most of the compounds compared to conventional
388 activated sludge biomass.
389
390 *4.2.2. Comparison between $K_{d,eq}$ and $K_{d,4h}$*
391 Sorption coefficients $K_{d,eq}$ were compared with $K_{d,4h}$ values for each chemical and relative
392 deviations Δ (%) between these two coefficients were calculated at different biofilm
393 thicknesses (Table 2) to verify the equilibrium assumption within the experiment duration (4
394 hours). For most compounds, relative deviations for Z50 and Z200 were on average around
395 10%, with the exception of atenolol (>50%). Conversely, Δ values in Z500 were – for most of
396 the eight compounds – higher than 30% (up to 80% for atenolol).
397 Overall, while the assumption of equilibrium reached within 4 h seems justified for Z50 and
398 Z200, diffusive mass transfer can significantly influence observations at higher biofilm

399 thickness. Atenolol was the main exception, for which the 4-h equilibrium assumption seems
400 not valid at any biofilm thickness. On the contrary, propranolol appeared to reach partitioning
401 equilibrium within 4-h in Z50, Z200 and Z500, and similar considerations could be made for
402 citalopram and venlafaxine. Therefore, to reduce uncertainties in sorption experiments,
403 parameter estimation can benefit from calculating the asymptotic aqueous concentration value
404 using e.g., simplified first-order decay equations (Eq. 4).
405
406 *4.2.3. Comparison between $K_{d,eq}$ and $K_{d,sups}$ and trends with biofilm thickness*
407 To assess the impact of biofilm porosity and mass transfer in pores on sorption coefficient
408 estimation, the sorption coefficients $K_{d,eq}$ and $K_{d,susp}$ were compared (Table S4). In Fig. 2, this
409 comparison is presented for two key chemicals (a: metoprolol, b: roxithromycin). For all
410 micropollutants, neglecting the transport from bulk aqueous phase to biofilm pores resulted in
411 an overestimation of sorption coefficients ($K_{d,susp}$ always greater than $K_{d,eq}$). The relative
412 deviation between $K_{d,susp}$ and $K_{d,eq}$ was on average ≤10% for most compounds and 30% for less
413 sorptive compounds (metoprolol and venlafaxine).
414 We further observed that both $K_{d,eq}$ and $K_{d,susp}$ generally increased with increasing biofilm
415 thickness (Fig. 2). Specifically, $K_{d,eq}$ values in Z500 were from 4-fold (most of the compounds)
416 up to 30-fold higher (macrolides antibiotics) than in Z50 (Table 2). It should be highlighted
417 that batch experiments were carried out at the same biomass concentration in the reactors (0.8
418 g L^{-1}). Consequently, the observed $K_{d,eq}$ increase with biofilm thickness likely derives from
419 differences in biofilm composition and/or in its physical properties. Two possible explanations
420 of this observation were proposed:
421 (i) Biomass composition, such as the relative fraction of autotrophic and heterotrophic bacteria
422 and/or the content of extracellular polymeric substances (EPS), can influence sorption

423 properties. EPS protein content was previously positively correlated with K_d for aromatic
424 chemicals in untreated and treated sewage sludge and colloids (Barret et al., 2010) and for the
425 estrogen EE2 and trimethoprim in nitrifying and heterotrophic biomass (Khunjar and Love,
426 2011). Bassin et al., (2012) further observed higher concentration of proteins and
427 polysaccharides (that mainly compose EPS) in heterotrophic MBBRs than in nitrifying
428 MBBRs. Higher fractions of heterotrophic bacteria (determined using quantitative PCR of 16S
429 rRNA) were measured in Z200 and Z500 compared to Z50 (Torresi et al., 2016), possibly
430 justifying the increased sorption capacity in thicker biofilms (Z200, Z500). Further
431 investigation on the EPS content in the different biofilms is thus required to support this
432 hypothesis, given the key role of EPS in the sorption of neutral and ionizable organic
433 chemicals (Späth et al., 1998; Barret et al., 2010; Khunjar and Love, 2011).
434 (ii) Porosity can influence the available surface area inside the biofilm. Sorption has been
435 previously positively impacted by reduced particle size, i.e., greater surface area, in suspended
436 biomass (Khunjar and Love, 2011) and biomass floc suspension derived from MBRs (Yi and
437 Harper, 2007). Thicker biofilms, having lower biomass density and substantially higher
438 porosity than thin biofilms, could accordingly provide for higher available surface (and thus
439 more accessible sites) for solid-liquid partitioning.
440 Finally, $K_{d,eq}$ values were normalized to the highest value of $K_{d,eq}$ (i.e., for Z500, $K_{d,eqZ500}$). The
441 obtained profiles followed two distinct trends as a function of biofilm thickness (Fig. 2c–d): (i)
442 beta-blockers and venlafaxine, exhibiting a logarithmic-like increase between Z50 and Z500;
443 and (ii) macrolides and citalopram, presenting significantly higher values for Z500, thus an
444 exponential-like increase of $K_{d,eq}$ with thickness. The question arises as to the influence of the
445 specific chemical properties of micropollutants on partitioning in biofilms, which was further
446 assessed using correlation analysis (see 4.5.2).

447 **< Figure 2 >**

448

449 ***4.3. Modelling diffusion and sorption in biofilm***

450 Based on the considerations above, calculated $K_{d,eq}$ were used to calibrate the diffusion-
451 sorption model against experimental data for the estimation of the dimensionless effective
452 diffusivity coefficient f (the only parameter estimated with the model). Simulated aqueous
453 concentrations (continuous lines, Fig. 3) predicted reasonably well the measured
454 concentrations in bulk liquid (circles, Fig. 3) for most of the targeted compounds (i.e., for
455 propranolol, clarithromycin, erythromycin, roxithromycin, citalopram, venlafaxine $R^2 > 0.9$;
456 Table S5). For atenolol, measured concentrations were less well predicted for Z50 and Z500
457 (R^2 equal to 0.8).

458 The simulated micropollutant concentrations in the bulk liquid and in the biofilm pores liquid
459 (dashed lines, Fig. 3) should converge when partitioning equilibrium is reached. This
460 equilibrium condition was satisfied for most compounds in Z50 and Z200 within 4 h
461 experimental time, with an average 10% relative deviation between simulated concentrations in
462 bulk and in biofilm pores. For the thickest biofilm (Z500), however, model predictions for
463 most of targeted chemicals suggested that equilibrium was not reached within 4 h (60%
464 average discrepancy with the last measurement). It is likely that, due to the greater thickness,
465 increased time to diffuse in deeper biofilm and thus to achieve sorption equilibrium is required
466 in Z500. The exception was propranolol, for which equilibrium seemed to be reached in all the
467 three biofilms, thus supporting results (relative deviation between $K_{d,4h}$ and $K_{d,eq}$) presented in
468 Table 2. For macrolide antibiotics, this discrepancy was significant and simulation results
469 suggested a time for partitioning equilibrium of approximately 10 days—in good agreement
470 with equilibrium times (days, months and years) in other environmental matrices (Delle Site,

2001). Furthermore, the large molecular volume and weight of macrolides (2- to 3-fold higher than the other targeted compounds, Table S2), as well as their high sorption potential in Z500, suggest slower diffusive transport inside the biofilm, as previously observed for hydrophobic organic molecules in sediments and soil (Wu and Gschwend, 1986).

There is a large variability concerning the time to reach partitioning equilibrium for organic chemicals in biofilms (Alvarino et al., 2015; Headley et al., 1998; Shi et al., 2011; Wicke et al., 2008; Writer et al., 2011), with values ranging from, e.g., 4 to 80 h for biofilm of 0.1 mm thickness (Wicke et al., 2008). In conclusion, our observations conflict with the widely held assumption of significantly shorter period of time (i.e. minutes to 1–2 hours) necessary to reach equilibrium in activated sludge (e.g., Hörsing et al., 2011; Pomiès et al., 2013). This may be explained by differences in pore-scale (hydro)dynamic conditions in MBBRs and activated sludge reactors, resulting in more pronounced mass transfer limitation in MBBRs.

< Figure 3 >

4.4. Influence of biofilm and chemical properties on f and $K_{d,eq}$

4.4.1. Estimation of f and proposed empirical correlation

Values of the dimensionless effective diffusivity coefficient f estimated for the three biofilm thicknesses and the eight sorptive compounds are reported in Fig. 4. For most of the compounds, with the exception of roxithromycin, f decreased with biofilm density and thus increased with biofilm thickness and porosity (with f in Z500 significantly higher than in Z200 and Z50 for all the compounds, and f in Z200 significantly higher than Z50 for six compounds). In thinner biofilms (≤ 50 µm), the transport of micropollutants could thus be limited by the high biomass density and the reduced porosity. A number of regressions to estimate f of solutes in biofilms as a function of biofilm density or porosity have been

previously developed (Fan et al., 1990; Guimerà et al., 2016; Horn and Morgenroth, 2006; Zhang and Bishop, 1994a), suggesting a negative correlation between *f* and density. Selected regression profiles (i.e., Guimerà et al., 2016; Horn and Morgenroth, 2006; Zhang and Bishop, 1994a; see Table S6) are reported in Fig. S3 for comparison with our *f* estimations. In particular, Guimerá et al. (2016) observed strong mass transfer limitation ($f < 0.1$) for oxygen in biofilm with density greater than 50 gVSS L^{-1}, in close agreement with findings (specifically for Z50) presented in this study.

< Figure 4 >

In general, estimated *f* were lower than values calculated from proposed regressions (Guimerà et al., 2016; Horn and Morgenroth, 2006; Zhang and Bishop, 1994a) (Fig. S3). While these regressions were identified for solutes with lower molecular weight (< 100 g mol^{-1}) and high solubility (e.g., O_2, sodium chloride, sodium nitrate), lower values of *f* (~0.2) were reported for most organic solutes with larger molecular weight (e.g., sugars and fatty acids; Stewart, 2003, 1998).

Given the possible influence of chemical properties on micropollutant diffusivity, we evaluated the relationship between *f* and several physico-chemical descriptors (section 3.5). No specific correlation was observed between *f* and molecular volume and other descriptors (Fig. S4). We observed a positive correlation only between *f* and $\log K_{OW}$ of the targeted compounds (Fig. S5), while negative dependence was reported in literature for organic compounds (Headley et al., 1998; Wicke et al., 2007; Wu and Gschwend, 1986). Notably, in this study the correlation was found for less hydrophobic ($0.1 < \log K_{OW} < 3.7$) and positively charged compounds (differently from previous studies), for which electrostatic interactions may also have influenced transport and partitioning. Thus, an empirical correlation between *f*, biofilm density ρ (as function of biofilm thickness) and $\log K_{OW}$ is proposed (Eq. 7):

519 $$f = \frac{1}{488 \cdot e^{-0.0072 L_F}} \ln\left(\frac{-12.7 - \log K_{OW,\max}}{\log K_{ow} - \log K_{OW,\max}}\right) \quad \text{(Eq. 7)}$$

520 where L_F is the biofilm thickness (µm) and log $K_{OW,max}$ is the asymptotic log $K_{OW,}$
521 approximating the highest value for the compounds selected. Profiles of f deriving from Eq. 7
522 were then depicted in Fig. 5, along with the estimated f values for the three biofilm thickness
523 (symbols, see also Fig. 4). Further details on the formulation of Eq. 7 are given in the SI
524 (section S4). We note that the size of the available data set may not be sufficiently large to
525 validate the correlation, and additional experimental evidence (higher biofilm thickness, wider
526 range of log K_{OW}) may be required for further confirmation.

527 **< Figure 5 >**

528

529 *4.4.2. Predictors of micropollutant $K_{d,eq}$ in biofilms*

530 Correlation analyses were performed between $K_{d,eq}$ and a number of physico-chemical
531 micropollutant descriptors.

532 First, the octanol-water partitioning coefficient of the neutral species (logK_{OW}) and the species-
533 dependent octanol-water distribution coefficient (log$D$) were assessed, exhibiting insignificant
534 correlation with $K_{d,eq}$ (-0.27 < Pearson's r < 0.15 for the three biofilms). This finding confirms
535 the limited reliability of logK_{OW} and log$D$ as sorption predictors for organic cations, as
536 previously shown in soil (Tolls, 2001; Franco and Trapp, 2008; Droge and Gross, 2013a).

537 Following this preliminary assessment, correlations with physico-chemical descriptors for
538 ionizable compounds (i.e., logpK_a, nrB, MV, log$TPSA$, log$vdWA$, V_X) were investigated (Fig. 6
539 and S6). Correlations for biofilm Z50 was performed only considering six compounds ($K_{d,eq}$ =
540 0 for venlafaxine and roxithromycin).

No significant correlations were found with the stereochemistry parameter *nRB* and logpK_a (Fig.S6). While previous studies positively correlated the sorption of cationic compounds with pK_a (r^2=0.5) (Franco and Trapp, 2008), the narrow range of pK_a values covered in this study prevented us from concluding on the significance of this indicator.

Interestingly, our analysis revealed a significant positive correlation only for Z500 between log$K_{d,eq}$ and log*TPSA*, log*vdWA,* McGowan's V_X (Fig. 6) and *MV* (Fig. S6a). The parameter *TPSA* was previously identified as sorption predictor only for neutral and negatively charged compounds, although with a negative correlation (Sathyamoorthy and Ramsburg, 2013). *TPSA* reflects the polarity of the organic chemical by accounting for the oxygen and nitrogen atoms, and the significance of the correlation thus suggests (at least for thicker biofilm) the strong contribution of the polar fraction on the sorption of positively charged compounds.

On the other hand, the positive correlation of log$K_{d,eq}$ with log*vdWA*, *MV* and V_X still suggests a contribution of hydrophobicity in sorption of positively charged compounds in Z500 biofilm. This finding is in line with previously established regressions for the prediction of distribution coefficients based on van der Waals volume (Kamlet et al., 1998) or V_X (Abraham, 1993; Abraham and Acree, 2010; Droge and Goss, 2013a,b,c) for neutral and ionized molecules. Notably, McGowan's volume positively correlates with van der Waals volume (Zhao et al., 2003), which is itself correlated to *vdWA*. Hence, both *vdWA* and V_X provide an indication of the influence of the molecular size in the cavity formation mechanism, through which solute molecules can distribute to an organic phase at the expenses of (i.e., by replacing) water molecules.

Considering the relevance of the correlation between log$K_{d,\mathrm{eq}}$ and V_X for Z500, an empirical regression model (Eq. 8) was tested based on the equation previously proposed by Droge and Goss (2013a,c) for sorption prediction of organic cations to soil organic matter:

$$\log K_{d,eq} = a \cdot V_X / 100 + b \cdot NA_i + c \quad \text{(Eq. 8)}$$

where $K_{d,eq}$ is expressed in L kg^{-1} and NA_i indicates the number of hydrogen atoms bound to the charged nitrogen moiety. The coefficients *a*, *b* and *c* were estimated by fitting Eq. 8 to measured sorption coefficients. The comparison between predicted and measured log$K_{d,eq}$ for Z500 is shown in Fig. 6d (*a*=0.35; *b*=0.44; *c*=1.49). The regression (r^2 = 0.59) could only partly describe sorption of cationic micropollutants in Z500 biofilms, yielding rather good $K_{d,eq}$ predictions (within factor 1.5 from measurements) for propranolol, clarithromycin, erythromycin and roxythromycin. Potential improvement of sorption predictions may be expected from the identification of correction factors for polar functional groups—an area beyond the scope of this study due to the limited number of substances.

Overall, results from this assessment confirm the challenges in the identification of unique and reliable sorption predictors for positively charged micropollutants in biofilm, as previously recognized for other matrices (Kah and Brown, 2007; Franco and Trapp, 2008; Franco et al., 2009; Sathyamoorthy and Ramsburg, 2013; Droge and Goss, 2013a,c; Bittermann et al., 2016). Nevertheless, it should be highlighted that in this study sorption was consistently observed only for positively charged compounds, indicating that electrostatic interaction with negatively charged biomass surfaces play a major role for sorption in biofilms.

< Figure 6 >

5. Conclusions

This study investigated the sorption and the diffusion of selected micropollutants in nitrifying MBBR biofilms (thickness=50, 200, 500 µm) by means of targeted experiments and process modelling, leading to the following conclusions:

- Sorption in biofilm occurred only for eight positively charged micropollutants (i.e.,

three macrolides, three beta-blockers and two psycho-active pharmaceuticals) out of 23 targeted substances. Electrostatic interaction with the negatively charged biomass surfaces appears to play a major role in the sorption to biofilms.

- Values of the partitioning coefficient $K_{d,eq}$ increased with increasing biofilm thickness for most of the sorbed compounds, being related to the increasing biofilm porosity and thus the higher surface area accessible for sorption. Sorption equilibria were reached within the duration of sorption experiments (4 h) for a number of compounds in 50 and 200 µm thick biofilms, but not in the thickest biofilm. Slower equilibrium in thick biofilms (≥500 µm) is likely determined by the longer time required to diffuse in deeper biofilm.
- Dimensionless effective diffusivity coefficients *f* for micropollutants (estimated for the first time in wastewater treatment biofilms) were negatively correlated with biofilm density, while showing an increase with increasing porosity. This indicates that diffusive transport may be strongly limited by the higher biomass density (and the lower porosity) of thinner biofilms.
- Significant positive correlations were observed between $logK_{d,\mathrm{eq}}$ and a limited number of chemical properties of micropollutants (topological polar surface area, van der Waals area and McGowan´s volume) but not for all biofilm thicknesses, confirming the challenges in the prediction of sorption in biofilms and other matrices for positively charged compounds.

Acknowledgments

This research was also supported by MERMAID, ITN funded by the People Programme (Marie Skłodowska-Curie Actions) of the EU FP7/2007-2013/ under REA grant agreement n°

607492'. F. Polesel and S. Trapp gratefully acknowledge the project LRI-ECO32 RABIT, funded under the CEFIC Long Range Research Initiative.

615 **References**

616 Abegglen, C., Joss, A., McArdell, C.S., Fink, G., Schlüsener, M.P., Ternes, T.A., Siegrist, H.,
617 2009. The fate of selected micropollutants in a single-house MBR. Water Res. 43, 2036–
618 46.
619 Abraham, M.H., McGowan, J.C., 1987. The use of characteristic volumes to measure cavity
620 terms in reversed phase liquid chromatography. Chromatogr. 23, 243–246.
621 Abraham, M.H., 1993. Scales of solute hydrogen-bonding: Their construction and application
622 to physicochemical and biochemical processes. Chem. Soc. Rev. 22, 73–83.
623 Abraham, M.H., Acree Jr., W.E., 2010. Equations for the transfer of neutral molecules and
624 ionic species from water to organic phases. J. Org. Chem. 75, 1006–1015
625 Alvarino, T., Suarez, S., Katsou, E., Vazquez-Padin, J., Lema, J.M., Omil, F., 2015. Removal
626 of PPCPs from the sludge supernatant in a one stage nitritation/anammox process. Water
627 Res. 68, 701–709.
628 Andersen, H.R., Hansen, M., Kjølholt, J., Stuer-Lauridsen, F., Ternes, T., Halling- Sørensen,
629 B., 2005. Assessment of the importance of sorption for steroid estrogens removal during
630 activated sludge treatment. Chemosphere 61, 139–146.
631 Barret, M., Carrère, H., Latrille, E., Wisniewski, C., Patureau, D., 2010. Micropollutant and
632 sludge characterization for modeling sorption equilibria. Environ. Sci. Technol. 44, 1100–
633 1106.
634 Barret, M., Carrere, H., Patau, M., Patureau, D., 2011. Kinetics and reversibility of
635 micropollutant sorption in sludge. J. Environ. Monit. 13, 2770–2774.
636 Bassin, J.P., Kleerebezem, R., Rosado, A.S., van Loosdrecht, M.C.M., Dezotti, M., 2012.
637 Effect of different operational conditions on biofilm development, nitrification, and
638 nitrifying microbial population in moving-bed biofilm reactors. Environ. Sci. Technol. 46,

639 1546–1555.
640 Beyenal, H., Lewandowski, Z., 2005. Modeling mass transport and microbial activity in
641 stratified biofilms. Chem. Eng. Sci. 60, 4337–4348.
642 Berthod, L., Whitley, D.C., Roberts, G., Sharpe, A., Greenwood, R., Mills, G.A., 2017.
643 Quantitative structure-property relationships for predicting sorption of pharmaceuticals to
644 sewage sludge during waste water treatment processes. Sci. Total Environ. 579, 1512–
645 1520.
646 Bittermann, K., Spycher, S., Goss, K.U., 2016. Comparison of different models predicting the
647 phospholipid-membrane water partition coefficients of charged compounds. Chemosphere
648 144, 382–391.
649 Brockmann, D., Rosenwinkel, K.H., Morgenroth, E., 2008. Practical identifiability of
650 biokinetic parameters of a model describing two-step nitrification in biofilms. Biotechnol.
651 Bioeng. 101, 497–514.
652 Clesceri, L.S., 1989. Standard methods for the examination of water and wastewater. American
653 Public Health Association.
654 Converti, A., Del Borghi, M., Zilli, M., 1997. Evaluation of phenol diffusivity through
655 Pseudomonas putida biofilms: Application to the study of mass velocity distribution in a
656 biofilter. Bioprocess Eng. 16, 105–114.
657 Cumming, G., Fidler, F., Vaux, D.L., 2007. Error bars in experimental biology. J. Cell Biol.
658 177, 7–11.
659 Delle Site, A., 2001. Factors affecting sorption of organic compounds in natural sorbent/water
660 systems and sorption coefficients for selected pollutants. A review. J. Phys. Chem. Ref.
661 Data 30, 187–439.
662 Droge, S.T.J., Goss, K.U., 2013a. Ion-exchange affinity of organic cations to natural organic

663 matter: Influence of amine type and nonionic interactions at two different pHs. Environ.
664 Sci. Technol. 47, 798–806.
665 Droge, S.T.J., Goss, K.U., 2013b. Sorption of organic cations to phyllosilicate clay minerals:
666 CEC normalization, salt dependency, and the role of electrostatic and hydrophobic effects.
667 Environ. Sci. Technol. 47, 14224−14232.
668 Droge, S.T.J., Goss, K.U., 2013c. Development and evaluation of a new sorption model for
669 organic cations in soil: Contributions from organic matter and clay minerals. Environ. Sci.
670 Technol. 47, 14233−14241.
671 Escolà Casas, M.E., Chhetri, R.K., Ooi, G., Hansen, K.M.S., Litty, K., Christensson, M.,
672 Kragelund, C., Andersen, H.R., Bester, K., 2015. Biodegradation of pharmaceuticals in
673 hospital wastewater by staged Moving Bed Biofilm Reactors (MBBR). Water Res. 83,
674 293–302.
675 Falås, P., Longrée, P., la Cour Jansen, J., Siegrist, H., Hollender, J., Joss, A, 2013.
676 Micropollutant removal by attached and suspended growth in a hybrid biofilm-activated
677 sludge process. Water Res. 47, 4498–4506.
678 Fan, L.S., Leyva-Ramos, R., Wisecarver, K.D., Zehner, B.J., 1990. Diffusion of phenol
679 through a biofilm grown on activated carbon particles in a draft-tube three-phase
680 fluidized-bed bioreactor. Biotechnol. Bioeng. 35, 279–286.
681 Fernandez-Fontaina, E., Omil, F., Lema, J.M., Carballa, M., 2012. Influence of nitrifying
682 conditions on the biodegradation and sorption of emerging micropollutants. Water Res.
683 46, 5434–5444.
684 Franco, A., Fu, W., Trapp, S., 2009. Influence of soil pH on the sorption of ionizable
685 chemicals: modeling advances. Environ. Toxicol. Chem. 28, 458–464.
686 Franco, A., Struijs, J., Gouin, T., Price, O.R., 2013. Evolution of the sewage treatment plant

687 model SimpleTreat: Applicability domain and data requirements. Integr. Environ. Assess.
688 Manag. 9, 1–32.
689 Franco, A., Trapp, S., 2008. Estimation of the soil-water partition coefficient normalized to
690 organic carbon for ionizable organic chemicals. Environ. Toxicol. Chem. 27, 1995–2004.
691 Göbel, A., Thomsen, A., McArdell, C.S., Joss, A., Giger, W., 2005. Occurrence and sorption
692 behavior of sulfonamides, macrolides, and trimethoprim in activated sludge treatment.
693 Environ. Sci. Technol. 39, 3981–3989.
694 Guimerà, X., Dorado, A.D., Bonsfills, A., Gabriel, G., Gabriel, D., Gamisans, X., 2016.
695 Dynamic characterization of external and internal mass transport in heterotrophic biofilms
696 from microsensors measurements. Water Res. 102, 551–560.
697 Hamon, P., Villain, M., Marrot, B., 2014. Determination of sorption properties of
698 micropollutants: What is the most suitable activated sludge inhibition technique to
699 preserve the biomass structure? Chem. Eng. J. 242, 260–268.
700 Hayduk, W., Laudie, H., 1974. Prediction of diffusion coefficients for nonelectrolytes in dilute
701 aqueous solutions. AIChE J. 20, 611–615.
702 Headley, J. V., Gandrass, J., Kuballa, J., Peru, K.M., Gong, Y., 1998. Rates of sorption and
703 partitioning of contaminants in river biofilm. Environ. Sci. Technol. 32, 3968–3973.
704 Holden, P.A., Hunt, J.R., Firestone, M.K., 1997. Toluene diffusion and reaction in unsaturated
705 Pseudomonas putida biofilms. Biotechnol. Bioeng. 56, 656–670.
706 Horn, H., Morgenroth, E., 2006. Transport of oxygen, sodium chloride, and sodium nitrate in
707 biofilms. Chem. Eng. Sci. 61, 1347–1356.
708 Hörsing, M., Ledin, A., Grabic, R., Fick, J., Tysklind, M., Jansen, J. la C., Andersen, H.R.,
709 2011. Determination of sorption of seventy-five pharmaceuticals in sewage sludge. Water
710 Res. 45, 4470–4482.

711 Hu, M., Zhang, T.C., Stansbury, J., Neal, J., Garboczi, E.J., 2013. Determination of porosity
712 and thickness of biofilm attached on irregular-shaped media. J. Environ. Eng. 139, 923–
713 931.
714 Hyland, K.C., Dickenson, E.R. V, Drewes, J.E., Higgins, C.P., 2012. Sorption of ionized and
715 neutral emerging trace organic compounds onto activated sludge from different
716 wastewater treatment configurations. Water Res. 46, 1958–1968.
717 Joss, A., Andersen, H., Ternes, T., Richle, P.R., Siegrist, H., 2004. Removal of estrogens in
718 municipal wastewater treatment under aerobic and anaerobic conditions: consequences for
719 plant optimization. Environ. Sci. Technol. 38, 3047–3055.
720 Joss, A., Zabczynski, S., Göbel, A., Hoffmann, B., Löffler, D., McArdell, C.S., Ternes, T. a.,
721 Thomsen, A., Siegrist, H., 2006. Biological degradation of pharmaceuticals in municipal
722 wastewater treatment: Proposing a classification scheme. Water Res. 40, 1686–1696.
723 Kah, M., Brown, C.D., 2007. Prediction of the adsorption of lonizable pesticides in soils. J.
724 Agric. Food Chem. 55, 2312–2322.
725 Kamlet, M.J., Doherty, R.M., Abraham, M.H., Marcus, Y., Taft, R.W., 1988. Linear solvation
726 energy relationships. 46. An improved equation for correlation and prediction of
727 octanol/water partition coefficients of organic nonelectrolytes (including strong hydrogen
728 bond donor solutes). J. Phys. Chem. 92, 5244–5255.
729 Khunjar, W.O., Love, N.G., 2011. Sorption of carbamazepine, 17α-ethinylestradiol, iopromide
730 and trimethoprim to biomass involves interactions with exocellular polymeric substances.
731 Chemosphere 82, 917–922.
732 Lipinski, C.A., Lombardo, F., Dominy, B.W., Feeney, P.J., 1997. Experimental and
733 Computational Approaches to Estimate Solubility and Permeability in Drug Discovery
734 and Develop ment Settings. Adv. Drug Deliv. Rev. 23, 3–25.

735 Margot, J., Rossi, L., Barry, D.A., Holliger, C., 2015. A review of the fate of micropollutants
736 in wastewater treatment plants. Wiley Interdiscip. Rev. Water 2, 457–487.
737 Maurer, M., Escher, B.I., Richle, P., Schaffner, C., Alder, a C., 2007. Elimination of beta-
738 blockers in sewage treatment plants. Water Res. 41, 1614–1622.
739 Mackay, A.A., Vasudevan, D., 2012. Polyfunctional ionogenic compound sorption: Challenges
740 and new approaches to advance predictive models. Environ. Sci. Technol. 46, 9209–9223.
741 Ort, C., Gujer, W., 2008. Sorption and high dynamics of micropollutants in sewers. Water Sci.
742 Technol. 57, 1791–1797.
743 Piculell, M., Suarez, C., Li, C., Christensson, M., Persson, F., Wagner, M., Hermansson, M.,
744 Jonsson, K., Welander, T., 2016. The inhibitory effects of reject water on nitrifying
745 populations grown at different biofilm thickness. Water Res. 104, 292–302.
746 Plósz, B.G., Langford, K.H., Thomas, K. V, 2012. An activated sludge modeling framework
747 for xenobiotic trace chemicals (ASM-X): assessment of diclofenac and carbamazepine.
748 Biotechnol. Bioeng. 109, 2757–2769.
749 Plósz, B.G.Y., Leknes, H., Thomas, K. V, 2010. Impacts of competitive inhibition, parent
750 compound formation and partitioning behavior on the removal of antibiotics in municipal
751 wastewater treatment. Environ. Sci. Technol. 44, 734–742.
752 Polesel, F., Lehnberg, K., Dott, W., Trapp, S., Thomas, K. V, Plósz, B.G., 2015. Factors
753 influencing sorption of ciprofloxacin onto activated sludge: Experimental assessment and
754 modelling implications. Chemosphere 119, 105–111.
755 Pomiès, M., Choubert, J.-M., Wisniewski, C., Coquery, M., 2013. Modelling of micropollutant
756 removal in biological wastewater treatments: a review. Sci. Total Environ. 443, 733–748.
757 Radjenović, J., Petrović, M., Barceló, D., 2009. Fate and distribution of pharmaceuticals in
758 wastewater and sewage sludge of the conventional activated sludge (CAS) and advanced

759 membrane bioreactor (MBR) treatment. Water Res. 43, 831–841.
760 Rattier, M., Reungoat, J., Keller, J., Gernjak, W., 2014. ScienceDirect Removal of
761 micropollutants during tertiary wastewater treatment by biofiltration : Role of nitrifiers
762 and removal mechanisms. Water Res. 54, 89–99.
763 Reichert, P., 1994. Aquasim - a tool for simulation and data-analysis of aquatic systems. Water
764 Sci. Technol. 30, 21–30.
765 Reif, R., Besancon, A., Le Corre, K., Jefferson, B., Lema, J.M., Omil, F., 2011. Comparison of
766 PPCPs removal on a parallel-operated MBR and AS system and evaluation of effluent
767 post-treatment on vertical flow reed beds. Water Sci. Technol. 63, 2411–2417.
768 Sathyamoorthy, S., Ramsburg, C.A., 2013. Assessment of quantitative structural property
769 relationships for prediction of pharmaceutical sorption during biological wastewater
770 treatment. Chemosphere 92, 639–646.
771 Shi, Y.J., Wang, X.H., Qi, Z., Diao, M.H., Gao, M.M., Xing, S.F., Wang, S.G., Zhao, X.C.,
772 2011. Sorption and biodegradation of tetracycline by nitrifying granules and the toxicity
773 of tetracycline on granules. J. Hazard. Mater. 191, 103–109.
774 Sibley, S.D., Pedersen, J.A., 2008. Interaction of the macrolide antimicrobial clarithromycin
775 with dissolved humic acid. Environ. Sci. Technol. 42, 422–428.
776 Späth, R., Flemming, H.C., Wuertz, S. (1998). Sorption properties of biofilms. Water Sci.
777 Technol. 37, 207–210.
778 Stevens-Garmon, J., Drewes, J.E., Khan, S.J., McDonald, J.A., Dickenson, E.R. V, 2011.
779 Sorption of emerging trace organic compounds onto wastewater sludge solids. Water Res.
780 45, 3417–3426.
781 Stewart, P.S., 2003. Diffusion in Biofilms: why is diffusion an important process. J. Bacteriol.
782 185, 1485–1491.

783 Stewart, P.S., 1998. A review of experimental measurements of effective diffusive
784 permeabilities and effective diffusion coefficients in biofilms. Biotechnol. Bioeng. 59,
785 261–272.
786 Tchobanoglous G., Burton F., Stensel H., Wastewater Engineering: Treatment and Reuse, 4th
787 ed., Metcalf and Eddy, Inc., McGraw-Hill Company, New York, 2003.
788 Ternes, T.A., Herrmann, N., Bonerz, M., Knacker, T., Siegrist, H., Joss, A., 2004. A rapid
789 method to measure the solid-water distribution coefficient (K_d) for pharmaceuticals and
790 musk fragrances in sewage sludge. Water Res. 38, 4075–4084.
791 Tolls, J. 2001. Sorption of veterinary pharmaceuticals in soils: A review. Environ. Sci.
792 Technol. 35, 3397−3406
793 Torresi, E., Fowler, S.J., Polesel, F., Bester, K., Andersen, H.R., Smets, B.F., Plósz, B.G.,
794 Christensson, M., 2016. Biofilm Thickness Influences Biodiversity in Nitrifying
795 MBBRs—Implications on Micropollutant Removal. Environ. Sci. Technol., 50 (17),
796 9279–9288.
797 Tran, N.H., Urase, T., Kusakabe, O., 2009. The characteristics of enriched nitrifier culture in
798 the degradation of selected pharmaceutically active compounds. J. Hazard. Mater. 171,
799 1051–1057.
800 Trapp, S., Matthies, M., 1998. Transport and Transformation of Compounds in Soil, in:
801 Chemodynamics and Environmental Modeling. Springer-Verlag, Berlin, Germany.
802 Uhrich, S.R.W., Navarro, D.A., Zimmerman, L., Aga, D.S., 2014. Assessing antibiotic sorption
803 in soil: A literature review and new case studies on sulfonamides and macrolides. Chem.
804 Cent. J. 8, 1–12.
805 Vasiliadou, I.A., Molina, R., Martínez, F., Melero, J. a, 2014. Experimental and modeling
806 study on removal of pharmaceutically active compounds in rotating biological contactors.

807 J. Hazard. Mater. 274, 473–482.
808 Wanner, O., Reichert, P., 1996. Mathematical modeling of mixed-culture biofilms. Biotechnol.
809 Bioeng. 49, 172–184.
810 Wicke, D., Böckelmann, U., Reemtsma, T., 2007. Experimental and modeling approach to
811 study sorption of dissolved hydrophobic organic contaminants to microbial biofilms.
812 Water Res. 41, 2202–2210.
813 Wicke, D., Böckelmann, U., Reemtsma, T., 2008. Environmental influences on the partitioning
814 and diffusion of hydrophobic organic contaminants in microbial biofilms. Environ. Sci.
815 Technol. 42, 1990–1996.
816 Writer, J.H., Ryan, J.N., Barber, L.B., 2011. Role of biofilms in sorptive removal of steroidal
817 hormones and 4-nonylphenol compounds from streams. Environ. Sci. Technol. 45, 7275–
818 7283.
819 Wu, S.C., Gschwend, P.M., 1986. Sorption kinetics of hydrophobic organic compounds to
820 natural sediments and soils. Environ. Sci. Technol. 20, 717–725.
821 Wunder, D.B., Bosscher, V.A., Cok, R.C., Hozalski, R.M., 2011. Sorption of antibiotics to
822 biofilm. Water Res. 45, 2270–2280.
823 Xue, W., Wu, C., Xiao, K., Huang, X., Zhou, H., Tsuno, H., Tanaka, H., 2010. Elimination and
824 fate of selected micro-organic pollutants in a full-scale anaerobic/anoxic/aerobic process
825 combined with membrane bioreactor for municipal wastewater reclamation. Water Res.
826 44, 5999–6010.
827 Yi, T., Harper, W.F., 2007. The effect of biomass characteristics on the partitioning and
828 sorption hysteresis of 17alpha-ethinylestradiol. Water Res. 41, 1543–1553.
829 Zacarias, G.D., Ferreira, C.P., Velasco-Hernandez, J.X., 2005. Porosity and tortuosity relations
830 as revealed by a mathematical model of biofilm structure. J. Theor. Biol. 233, 245–251.

831 Zhang, S.F., Splendiani, A., Freitas dos Santos, L.M., Livingston, A.G., 1998. Determination
832 of pollutant diffusion coefficients in naturally formed biofilms using a single tube
833 extractive membrane bioreactor. Biotechnol. Bioeng. 59, 80–89.
834 Zhang, T.C., Bishop, P.L., 1994a. Evaluation of turtuosity factors and effective diffusivities in
835 biofilms. Water Res. 28, 2279–2287.
836 Zhang, T.C., Bishop, P.L., 1994c. Density, porosity, and pore structure of biofilms. Water Res.
837 28, 2267–2277.
838 Zhao, Y.H., Abraham, M.H., Zissimos, A.M., 2003. Determination of McGowan volumes for
839 ions and correlation with van der Waals volumes. J. Chem. Inf. Comput. Sci. 43, 1848–
840 1854.
841

842 Tables

843 **Table 1.** Biofilm characteristics and input parameters used in the sorption and diffusion model
844 in this study.

Parameter	Z50	Z200	Z500	Reference
Boundary layer thickness L_L (µm)	10	10	10	(Brockmann et al., 2008)
Dry biofilm mass per carrier (gTS m^{-2})	2.33	4.46	9.00	Measured
Biomass dry density in biofilm D_d (g cm^{-3})	1.17	1.05	1.05	Calculated
Porosity ε (%)	76	91	93	Calculated
Biofilm wet density ρ (kg m^{-3})	51	19	16	Calculated

845

846 **Table 1.** Sorption coefficients calculated according to final concentration at equilibrium ($K_{d,eq}$)
847 and according to last measured aqueous concentration after 4 h of batch experiment ($K_{d,4h}$) for
848 eight of the 22 spiked chemical compounds, exhibiting significant.

849

	Z50			Z200			Z500			
	$K_{d,eq}$ (L g^{-1})	$K_{d,4h}$ (L g^{-1})	Δ (%)	$K_{d,eq}$ (L g^{-1})	$K_{d,4h}$ (L g^{-1})	Δ (%)	$K_{d,eq}$ (L g^{-1})	$K_{d,4h}$ (L g^{-1})	Δ (%)	Literature K_d (L g^{-1})
Atenolol	1.12±2.21	0.26	77	1.10±0.34	0.68	38	4.72±0.73	0.95	80	(0.006)[1]-1.9[2]
Metoprolol	0.08±0.01	0.08	3	0.19±0.06	0.16	15	0.27±0.02	0.15	44	<0.01[3]-0.23[4]
Propranolol	0.50±0.04	0.54	-9	1.69±0.03	1.67	1	1.90±0.06	1.92	-1	0.2[1]-0.32[3]
Clarithromycin	0.42±0.11	0.34	20	0.41±0.02	0.39	4	10.90±0.25	5.63	48	0.26[5]-1.2[6]
Erythromycin	0.33±0.07	0.34	-3	0.19±0.01	0.20	-4	10.68±2.09	6.13	43	0.31[1]-1[7]
Roxithromycin	0.00	0.00	/	0.85±0.13	1.05	-24	10.80±0.32	3.92	64	<0.1[9]-0.5[6]
Citalopram	0.47±0.08	0.46	1	0.66±0.08	0.61	8	2.46±0.15	2.06	16	0.54[2]
Venlafaxine	0.00	0.00	/	0.12±0.05	0.09	25	0.14±0.06	0.12	16	<0.1[2]

850 [1] (Radjenović et al., 2009) for atenolol the lowest value was found in FS MBR; [2] (Hörsing et al., 2011) for atenolol in
851 secondary sludge; [3] (Maurer et al., 2007); [4](Sathyamoorthy et al., 2013); [5] (Göbel et al., 2005); [6] (Abegglen et al., 2009)
852 in MBR; [7] (Xue et al., 2010) in activated sludge and MBR; [9] (Fernandez-Fontaina et al., 2012).

853

Figures

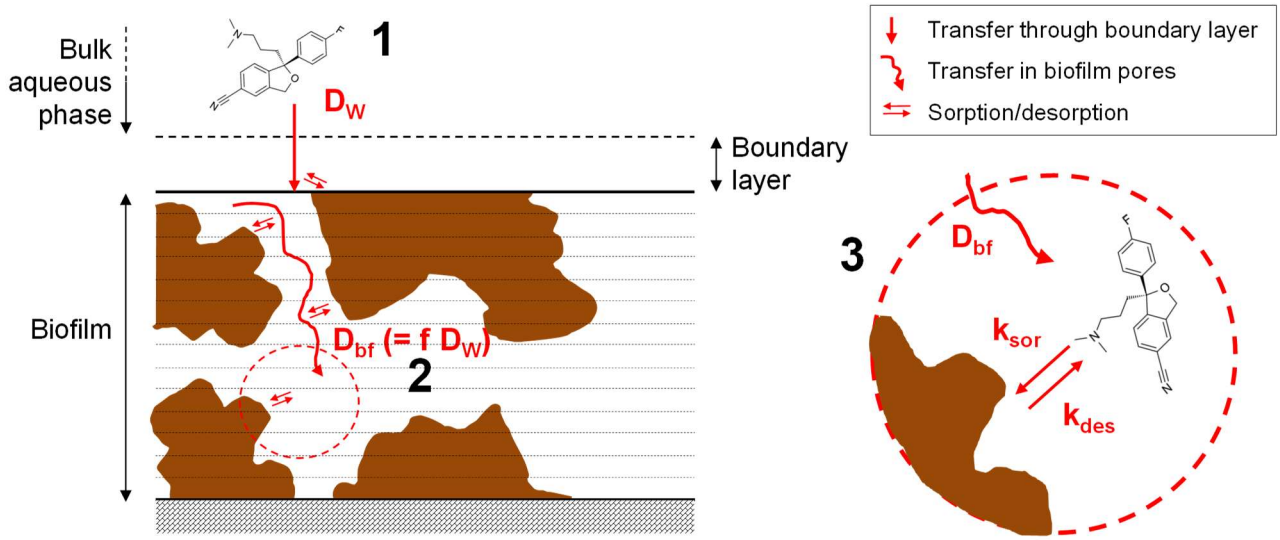

Assumptions

(i) Same diffusivity in bulk liquid and boundary layer

(ii) Biofilm is a homogeneous porous medium

(iii) Sorption to biofilm solid matrix is instantaneous, i.e. sorption kinetics limited by diffusion though boundary layer and biofilm pores

(iv) Sorption is assumed linear (K_d)

Process	Component		Process rate
	C_{LI}	C_{SL}	
Desorption	1	-1	$k_{des}C_{SL}$
Sorption	-1	1	$k_{des}K_dC_{LI}X$

Figure 1. Conceptual model for diffusion and sorption of micropollutants into biofilms, including the consecutive steps required for partitioning onto biofilm solids (processes 1–3, see text), the assumptions considered in the model and the process matrix describing sorption and desorption kinetics (X=$X_{biomass}$).

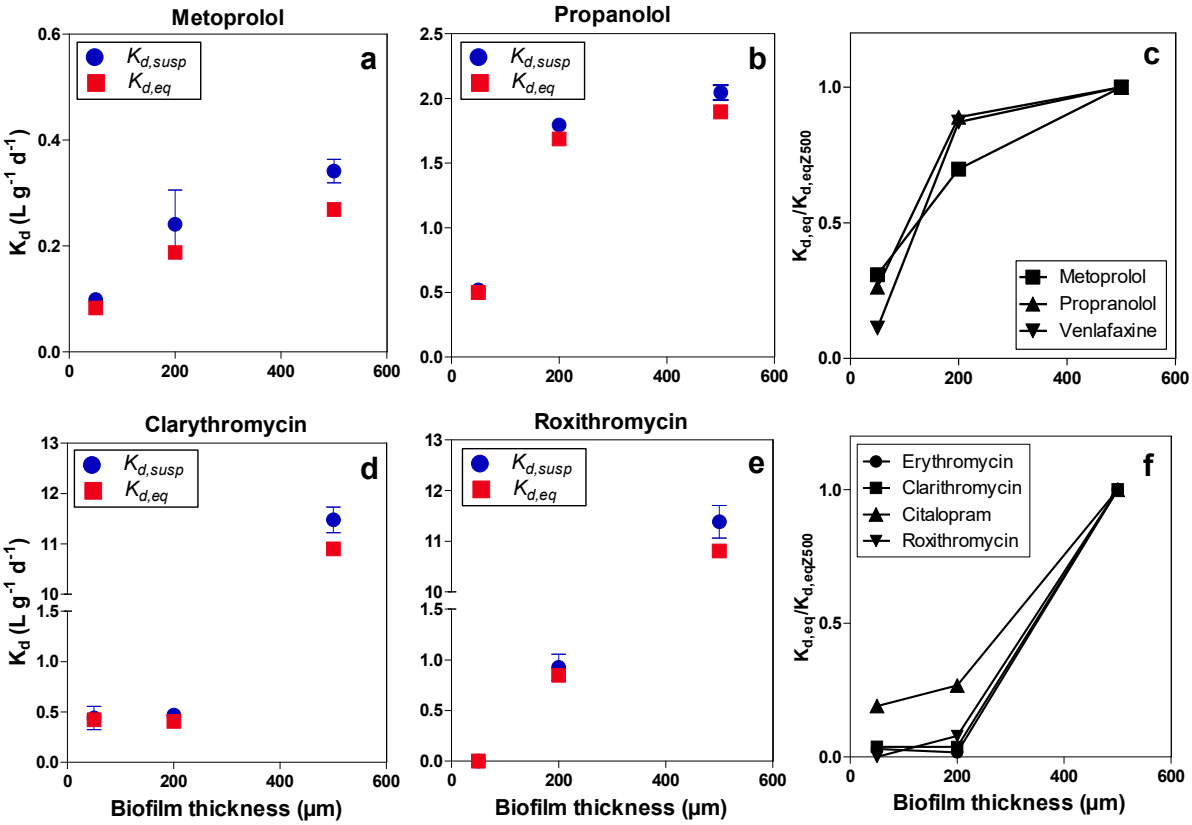

862

863 **Fig. 2.** Comparison between sorption coefficient accounting for diffusion (Kd_Suspended) and

864 not accounting for diffusion.

865

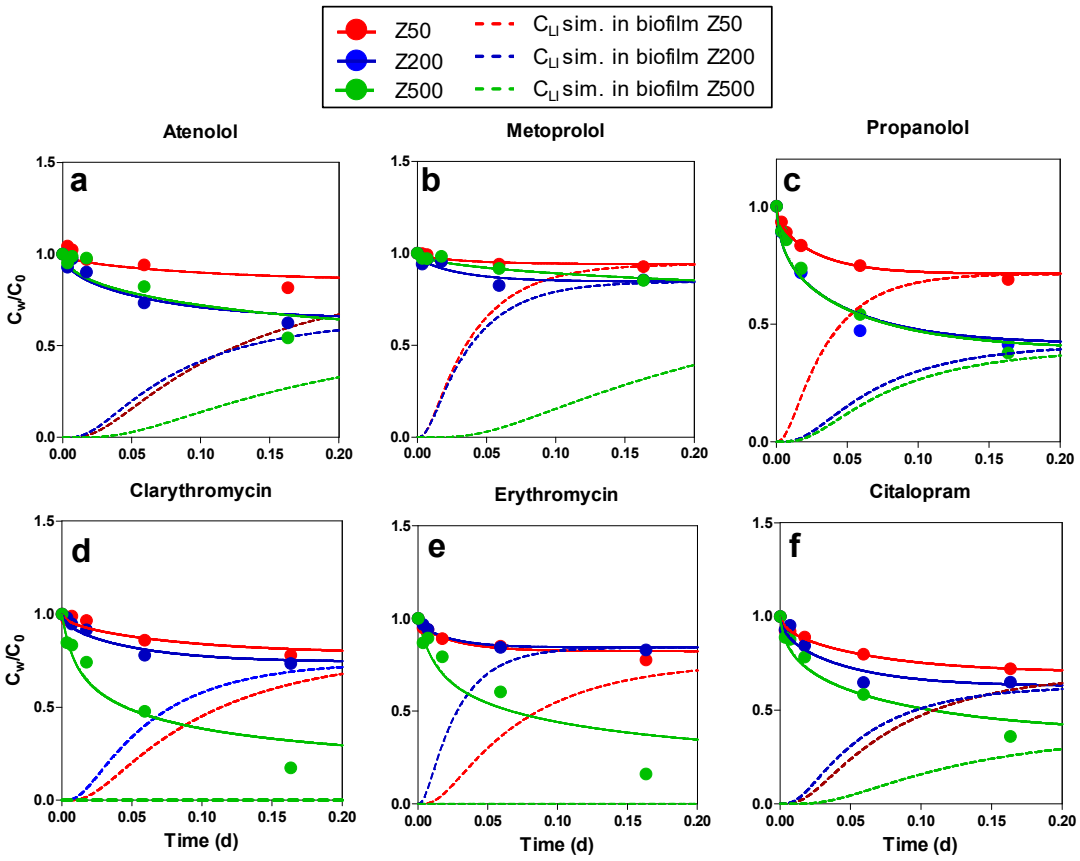

866

867 **Fig. 3.** Measured (circles) and simulated (continuous line) aqueous concentrations in bulk
868 aqueous phase and simulated concentrations in biofilm pores (dashed lines) of six selected
869 chemicals compounds during batch experiments with Z50 (red), Z200 (blue) and Z500 (green)
870 biofilms.

871

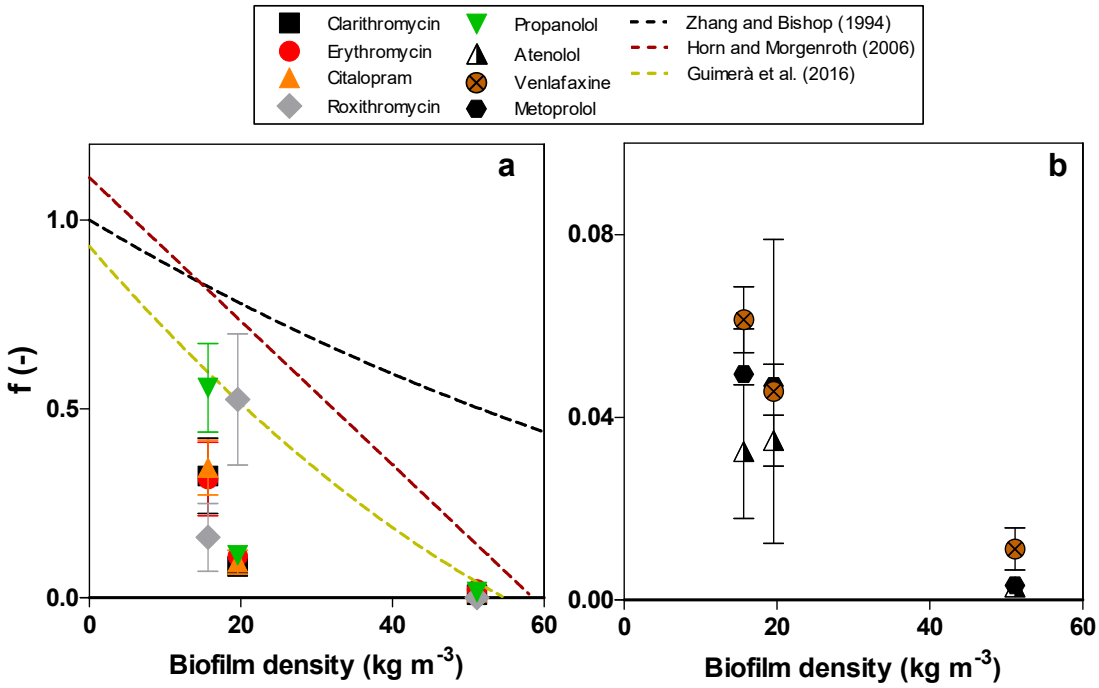

872

873 **Figure 4.** Estimated values of effective diffusivity for the three biofilm thickness and the

874

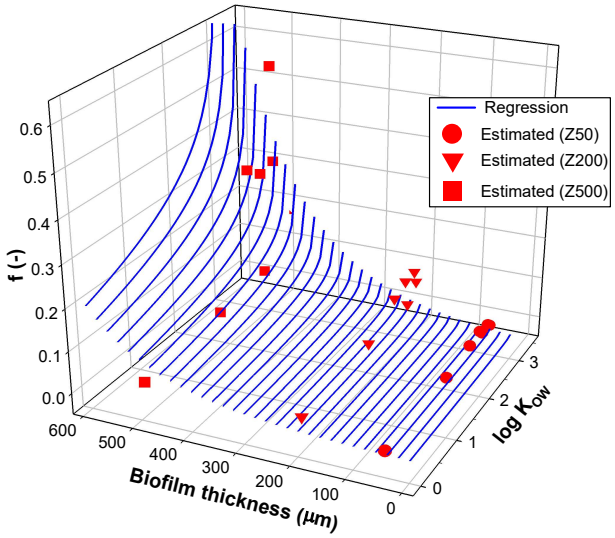

875

876 **Fig. 5.** Plots of the empirical equation describing *f* as a function of biofilm thickness and
877 logK_{ow}, together with estimated *f* values (red symbols) in Z50, Z200 and Z500.

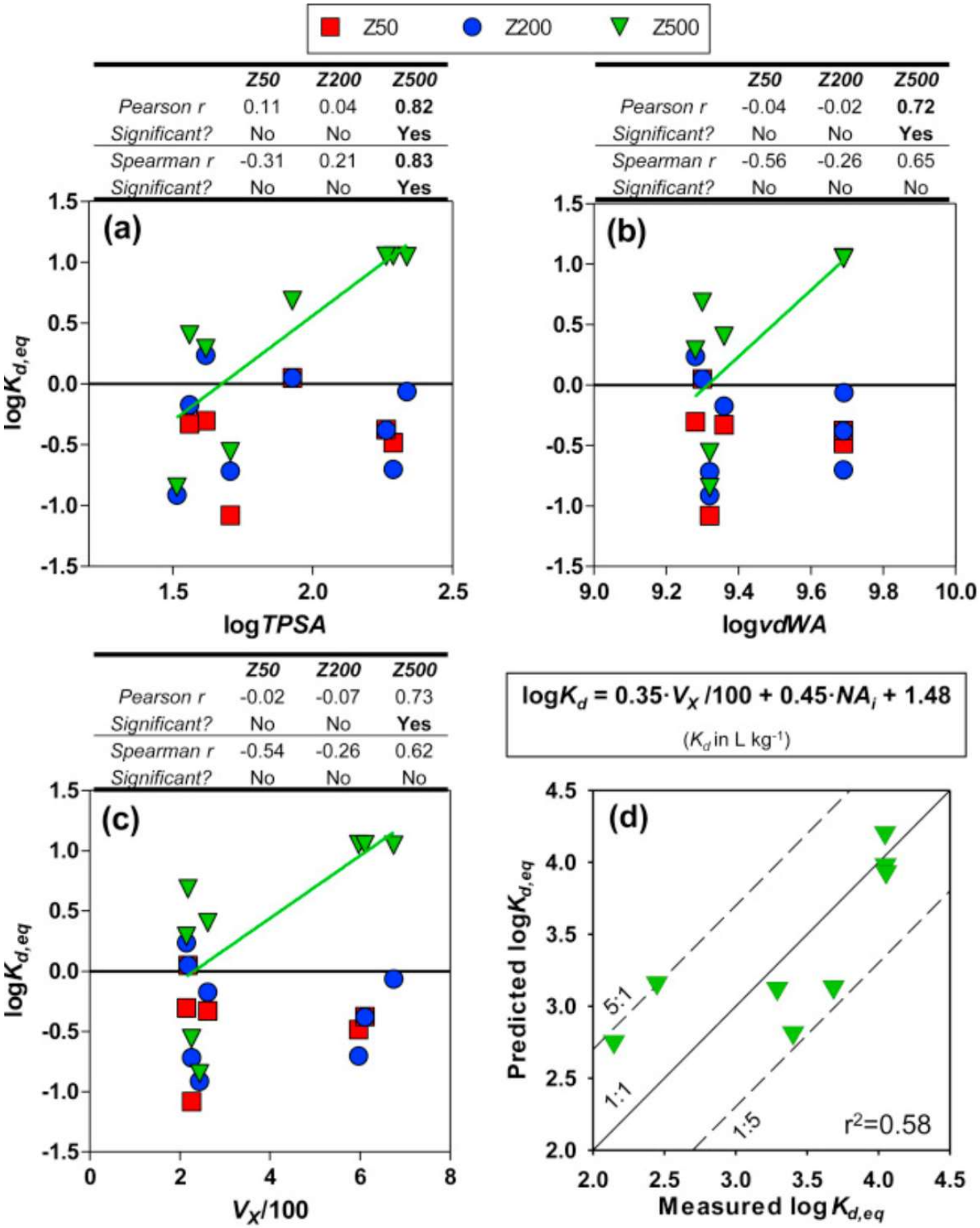

878

879 Fig. 6. Correlation analysis between logKd,eq of the targeted micropollutants for the

880 three biofilms (Z50, Z200, Z500) and physico-chemical descriptors: (a) logTPSA;

881 (b) log vdWA; (c) McGowan's volume VX (divided by a factor of 100). Linear
882 regression lines were reported only for significant correlations. Based on the
883 correlation with VX/100, an empirical regression (Eq. (8)) was tested according to
884 Droge and Goss (2013a, c). The comparison between measurements and predictions
885 using Eq. (8) (in both cases, with Kd,eq in L kg−1) is presented in (d).